Reconfigurable Control for Formation of Antennas in Earth Orbit

Fred Y. Hadaegh, Daniel P. Scharf, Scott R. Ploen and Vaharaz Jamnejad

Jet Propulsion Laboratory
California of Institute of Technology
Pasadena, CA 91109 USA
Hadaegh@jpl.nasa.gov

Abstract

An integrated control and electromagnetic/antenna formulation is presented for evaluating the performance of a distributed antenna system as a function of formation geometry. A distributed and self-organizing control law for the control of multiple antennas in Low Earth Orbit (LEO) is presented. The control system provides collaborative commanding and performance optimization to configure and operate the distributed formation system. A large aperture antenna is thereby realized by a collection of miniature sparse antennas in formation. A case study consisting of a simulation of four antennas in Low Earth Orbit (LEO) is presented to demonstrate the concept.
Keywords: Formation flying, Leader/Follower, Self-organizing, Sparse antenna, Formation control

1. Introduction

In recent years, the science community has been actively considering the use of distributed spacecraft for deep space and Earth science missions. One such application is to use a large number of small spacecraft in place of a large deployable antenna in order to achieve very large sparse apertures for Earth imaging (for example, at resolutions of ≈ 10 cm). Another application is the use of multiple telescopes flying in precision formation as an interferometer in deep space for stellar imaging and planet detection. A number of such missions have been proposed that offer unprecedented performance capabilities beyond the scope of any single large telescope [17,18]. Compared to their equivalent monolithic aperture counterparts, formation flying sparse antennas offer launch and deployment efficiency, and has the advantage of avoiding the structural complexity and pointing issues associated with large aperture, lightweight, antenna dishes in space.

This paper presents an integrated control and electromagnetic/antenna approach needed to realize, for the first time, distributed formation flying spacecraft antenna systems in Low Earth Orbit (LEO). The paper focuses on the core guidance and control (G&C) algorithms needed to perform parametric studies to access the impact of replacing a large monolithic space-based antenna by a collection of miniature spacecraft. This concept is shown in Figure 1. The development of techniques/algorithms to couple formation flying with 3-dimensional electromagnetic field pattern generation is another important objective of this paper. To this end, formation dynamics and environmental disturbance modeling is presented in Section 3. Formation guidance and control design for both translation and attitude are presented in Section 4 and 5. Section 6 provides analysis of a spatial array of antennas along with simulations. Section 7 presents a four-spacecraft sparse aperture example for evaluation of the distributed antenna system performance.

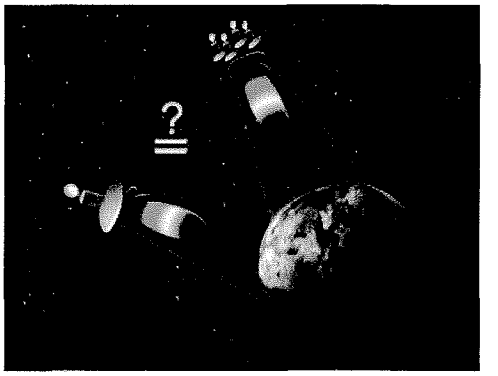

Figure 1. Can a few small antennas replace a larger antenna in space?

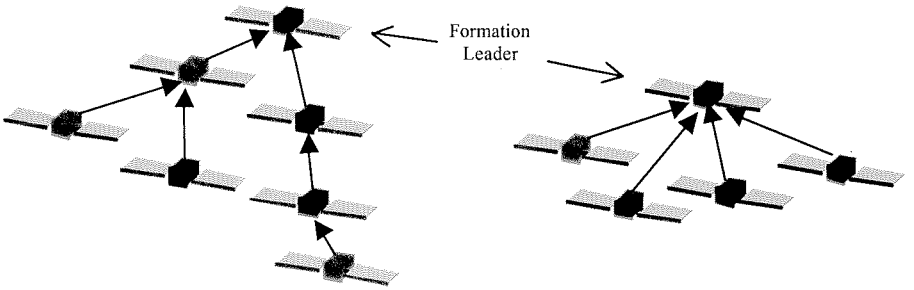

General L/F Architecture Single-Layer L/F Architecture

Figure 2. Two possible L/F architectures. Solid arrows indicate leader assignment.

2. Sparse Antenna Guidance and Control Architecture

In general, the methodology for coordination and control of spacecraft in a formation is strongly correlated with the formation size and particular application. In a completely centralized architecture, a single master spacecraft commands all aspects of the other slave spacecraft. At the other end of the spectrum is a completely decentralized architecture in which spacecraft interact locally with other nearby spacecraft. In this latter case, formation behavior is said to be "emergent," and is similar to the schooling of fish or the flocking of birds. The defining characteristic of a decentralized architecture is that individual spacecraft do not require knowledge of the entire formation state for control.

Here we use the Leader/Follower (L/F) decentralized control architecture [8] for controlling relative spacecraft *positions* (attitude control is discussed subsequently). This architecture is robust and scaleable (e.g., individual spacecraft failures do not affect the overall formation stability and additional spacecraft can be easily added using only local control design[1]). In the L/F architecture, individual spacecraft controllers are connected in a hierarchical fashion. With the exception of the formation leader discussed below, each spacecraft is assigned a leader that the spacecraft "follows," i.e., a follower spacecraft controls its position with respect to its leader. The leader may in turn be following another spacecraft. There is at least one spacecraft in the formation that does not follow another spacecraft. This spacecraft is referred to as the formation leader. The motion of the formation leader controls the motion of the entire formation. We initially consider small to medium formations (i.e., 5 to 10 spacecraft). In this case, a single-layer L/F architecture is feasible. Hence, all spacecraft follow the same spacecraft, which is the designated formation leader. For larger formations, single-layer L/F imposes restrictive inter-spacecraft communication and sensing requirements. Figure 2 shows examples of a general L/F architecture and a single-layer L/F architecture.

Absolute spacecraft attitudes are controlled independently so that individual apertures are pointed in the nadir direction.[2] A spacecraft's nadir direction is determined using real time inertial position knowledge obtainable from GPS measurements to 10 m (1σ) accuracy (we cannot use precision centimeter level orbit determination as was used for Topex/Poseidon since this position data is delayed by up to a day) [9]. For the orbits considered, a 10 m inertial positioning error leads to a maximum nadir pointing error of 0.1 arc-minutes. Therefore, inertial positioning errors can be ignored for our purposes.[3]

The formation guidance has a hybrid architecture; part centralized and part decentralized. The attitude guidance is decentralized; each spacecraft points its aperture in the nadir direction independently of the other spacecraft. The translational guidance is centralized. A path-planning algorithm on the formation leader plans the relative trajectories of each follower with respect to the formation leader. These trajectories are then communicated to the followers.

For a collection of spacecraft (apertures) to function cooperatively as a sparse antenna, the control system must be capable of maintaining specified relative

[1] To add or remove a spacecraft from a centralized formation control architecture, the entire formation controller must be redesigned.

[2] Another alternative to be evaluated is using L/F to point all spacecraft in the formation leader's nadir direction.

[3] GPS-based technologies are being developed that can sense inertial positions to the centimeter level in real time. These technologies have the capability of superceding carrier differential GPS-based measurements in the future.

spacecraft positions to a fraction of the antenna wavelength. As a result, scientific applications require *precision formation flying* (i.e., centimeter/arc-minute-level relative position/attitude control). Relative position requirements have been previously studied for synthetic aperture applications: In the VHF radio frequency band (i.e., 1 to 10 m wavelengths), relative spacecraft positions must be controlled to approximately the 15 cm level. Similarly, for interferometric synthetic aperture radar applications in the L band (15 to 30 cm wavelengths), relative spacecraft positions must be controlled to approximately the 3 cm level [1]. These relative positioning requirements are consistent with current carrier differential phase GPS (CDGPS) sensors, which can measure relative positions with 2 cm (1σ) of accuracy. Attitude requirements for radar and radio frequency synthetic apertures are not as well defined [2]; a spacecraft must only point to a fraction of an aperture's beam pattern width [3], which is application dependent.

In this paper, we assume that all the spacecraft are nadir-pointing (i.e., down-looking) and that the attitude control requirements are consistent with attitude sensing via CDGPS (i.e., 5 to 10 arcminute level)[10].

In summary, robust precision formation control and guidance algorithms must be developed that (1) maintain relative spacecraft positions and absolute attitudes to 5 cm and 10 arc-minutes, respectively, and that (2) reconfigure the formation using fuel-optimal, collision free trajectories. Further, these algorithms must perform over orbits with altitudes ranging from 250 to 1000 km and non-zero eccentricity.

3. Formation and Environmental Disturbance Models

A sparse antenna formation may be in a circular 200 km or an eccentric 1000 km orbit. The ambient formation dynamic environment varies widely over this range of possible orbits. For example, the relative spacecraft dynamics are time-invariant (to first order) for a circular orbit, but are time-varying for an eccentric orbit. Further, disturbances vary by orders of magnitude depending upon orbit semi-major axis and inclination. In the following section, the equations of motion for an N spacecraft formation of distributed antennas in LEO are presented followed by models for environmental disturbances.

3.1 Distributed Antennas Models

Each antenna is modeled as a rigid body with three translational and three rotational degrees-of-freedom. Each spacecraft is subjected to a pure Keplerian (i.e., two-body) gravitational potential along with environmental disturbances including perturbations due to J_2 oblateness effects, aerodynamic drag, solar radiation pressure, and Sun/Moon gravitational perturbations. We further assume that each spacecraft has full control authority in both translation and rotation along all axes. The orbital geometry of the formation is shown in Figure 3. Here the translational motion of spacecraft i relative to spacecraft j is described with respect to a Keplerian reference orbit where $\vec{R}_O$ denotes the reference orbit trajectory, and $\vec{\rho}_i$ denotes the position of the i^{th} spacecraft relative to the origin of the orbit reference frame. The linearized translational equations of motion of each spacecraft $i = 1,2,\ldots N$ valid for $|\vec{\rho}_i| \ll |\vec{R}_O|$ are given by

$$\ddot{\vec{R}}_O + \frac{\mu \vec{R}_O}{R_O^3} = \vec{0} \tag{1}$$

$$\ddot{\vec{\rho}}_i + \frac{\mu}{R_O^3}\left(\vec{I} - 3\hat{o}_1 \otimes \hat{o}_1\right)\vec{\rho}_i = \vec{a}_{oi} + \vec{a}_{pi} + \frac{1}{m_i}\left(\vec{F}_{ai} + \vec{F}_{si} + \vec{F}_{ci}\right) \tag{2}$$

Here the magnitude of $\vec{R}_O$ is denoted by R_O, $\{\hat{o}_1, \hat{o}_2, \hat{o}_3\}$ denotes the right-handed orthonormal triad defining the orbit reference frame shown in Figure 3 where $\hat{o}_1$ points nadir, $\hat{o}_2$ is normal to the plane of the reference orbit, and $\hat{o}_3$ completes the triad, μ denotes the gravitational parameter of the Earth, $\vec{I}$ denotes the unit dyadic, the symbol $\otimes$ denotes the tensor product, $\vec{a}_{oi}$ denotes the perturbation on the i^{th} spacecraft due to central-body oblateness effects, $\vec{a}_{pi}$ denotes the perturbation on the i^{th} spacecraft due to the gravitational attraction of the Sun and Moon, $\vec{F}_{ai}$ is the resultant aerodynamic force at the center-of-mass of the i^{th} spacecraft, $\vec{F}_{si}$ is the resultant solar radiation force acting at the center-of-mass of the i^{th} spacecraft, and $\vec{F}_{ci}$ denotes the control force applied to the center-of-mass of the i^{th} spacecraft. Note that all derivatives in the equations of motion are inertial derivatives.

The rotational equations of motion of each antenna $i = 1,2,\ldots N$ are given by

$$\dot{q}_i = \frac{1}{2}\Gamma(q_i)\vec{\omega}_i \tag{3}$$

$$\vec{J}_i\dot{\vec{\omega}}_i + [\vec{\omega}_i]\vec{J}_i\vec{\omega}_i = \vec{\tau}_{ai} + \vec{\tau}_{si} + \vec{\tau}_{ci} \tag{4}$$

where q_i denotes the unit quaternion describing the absolute attitude of the i^{th} spacecraft, Γ is the attitude dependent kinematic Jacobian matrix, $\vec{\omega}_i$ denotes the absolute angular velocity of the i^{th} spacecraft, $[\vec{\omega}_i]$ denotes the skew-symmetric cross product operator, $\vec{J}_i$ denotes the central inertia dyadic of the i^{th} spacecraft, $\vec{\tau}_{ai}$ denotes the resultant aerodynamic torque acting at the center-of-mass of the i^{th} spacecraft, $\vec{\tau}_{si}$ denotes the resultant solar radiation torque acting at the center-of-mass of the i^{th} spacecraft, and $\vec{\tau}_{ci}$ denotes the applied control torques at the center-of-mass of the i^{th} spacecraft.

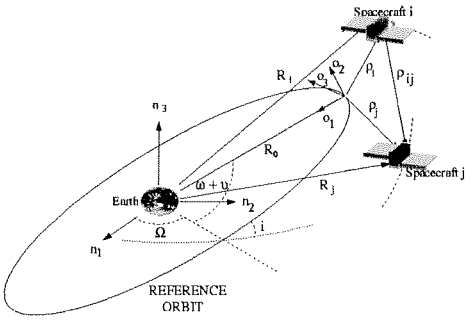

Figure 3. Orbital Geometry

3.2 Environmental Disturbance Models

In this section, the explicit form of the disturbance models appearing in the equations of motion are presented. First, the perturbation due to Earth oblateness effects on the i^{th} spacecraft is given by

$$\vec{a}_{oi} = -\frac{3\mu J_2 a^2}{2R_i^4}(c_{1i}\hat{e}_i + c_{2i}\hat{n}_3) \qquad (5)$$

where $c_{1i} = 1 - 5(\hat{e}_i \bullet \hat{n}_3)^2$, $c_{2i} = 2(\hat{e}_i \bullet \hat{n}_3)$, and the symbol $\bullet$ denotes the standard dot product. Also J_2 denotes the second zonal harmonic of the Earth, a is the mean radius of the Earth, $\hat{e}_i$ denotes a unit vector along the absolute position vector $\vec{R}_i$ of spacecraft i, R_i denotes the magnitude of $\vec{R}_i$, and $\hat{n}_3$ denotes the polar axis of the Earth. Note that the perturbation due to oblateness has components in both the radial and polar directions.

The perturbations on the i^{th} spacecraft due to third-body (e.g., Sun, Moon) gravitational interactions is given by

$$\vec{a}_{pi} = \sum_{j=1}^{N_p} \mu_j \left(\frac{\vec{r}_{1j} - \vec{R}_i}{r_{2j}^3} - \frac{\vec{r}_{1j}}{r_{1j}^3} \right) \qquad (6)$$

where μ_j is the gravitational parameter of the j^{th} perturbing body, N_p denotes the number of perturbing bodies and the vectors $\vec{r}_{1j}$ and $\vec{r}_{2j}$ are as shown in Figure 4.

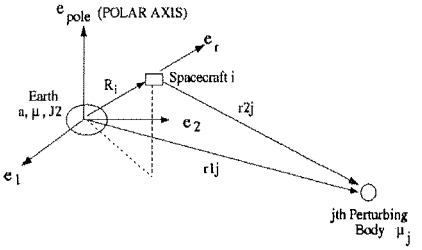

Figure 4. Geometry of Third-body Perturbations

The aerodynamic disturbances acting on a single spacecraft are modeled by approximating each spacecraft as a convex collection of flat faces. For simplicity we assume that all spacecraft are identical and consist of the same number of faces, denoted N_{face}. The resultant aerodynamic force and torque about the center of mass of the i^{th} spacecraft, denoted $\vec{F}_{ai}$ and $\vec{\tau}_{ai}$ respectively, are given by

$$\vec{F}_{ai} = \sum_{j=1}^{N_{face}} \eta_j \vec{F}_{aij} \qquad (7)$$

$$\vec{\tau}_{ai} = \sum_{j=1}^{N_{face}} \eta_j \vec{r}_{ij} \times \vec{F}_{aij} \qquad (8)$$

where

$$\vec{F}_{aij} = -\frac{1}{2} C_{d,ij} A_{ij} \rho V_{rel,ij}^2 (\hat{n}_{ij} \bullet \hat{V}_{rel,ij}) \hat{V}_{rel,ij} \qquad (9)$$

and

$$\vec{V}_{relij} = (\vec{V}_i + \vec{\omega}_i \times \vec{r}_{ij}) - \vec{\omega}_p \times (\vec{R}_i + \vec{r}_{ij}) \qquad (10)$$

Here $\vec{F}_{a,ij}$ denotes the resultant aerodynamic force acting on the j^{th} face of the i^{th} spacecraft, $\vec{r}_{ij}$ is the center-of-mass to center-of-pressure offset of the j^{th} face of the i^{th} spacecraft, η_j denotes a face participation factor, $C_{d,ij}$ denotes the drag coefficient of the j^{th} face of spacecraft i, A_{ij} denotes the area of the j^{th} face of the i^{th} spacecraft, ρ is the altitude-dependent atmospheric density, $\hat{n}_{ij}$ denotes the unit normal of the j^{th} face of the i^{th} spacecraft, $\vec{V}_{rel,ij}$ is the velocity of the j^{th} face of the i^{th} spacecraft relative to the atmosphere, $\hat{V}_{rel,ij}$ denotes a unit vector along $\vec{V}_{rel,ij}$, $\vec{V}_i$ is the absolute velocity of the center-of-mass of the i^{th} spacecraft, $\vec{\omega}_i$

denotes the absolute angular velocity of spacecraft i, $\vec{R}_i$ is the absolute position of the center-of-mass of the i^{th} spacecraft, and $\vec{\omega}_p$ denotes the absolute angular velocity of the Earth. Note that we have assumed the atmosphere rotates with the same angular velocity as the Earth.

The disturbance due to solar radiation pressure acting on a single spacecraft is also computed by approximating each spacecraft as a collection of flat faces. The resultant force and torque about the center of mass of the i^{th} spacecraft due to solar radiation pressure, denoted $\vec{F}_{si}$ and $\vec{\tau}_{si}$ respectively, are given by

$$\vec{F}_{si} = \sum_{j=1}^{N_{face}} \eta_j \vec{F}_{s,ij} \tag{11}$$

$$\vec{\tau}_{si} = \sum_{j=1}^{N_{face}} \eta_j \vec{r}_{ij} \times \vec{F}_{s,ij} \tag{12}$$

where

$$F_{s,ij} = -PA_{ij}(\hat{n}_{ij} \bullet \hat{s}_{ij})[(1-c_{s,ij})\hat{s}_{ij} + 2\{c_{s,ij}(\hat{n}_{ij} \bullet \hat{s}_{ij}) + \frac{1}{3}c_{d,ij}\}\hat{n}_{ij}] \tag{13}$$

Here $\hat{s}_{ij}$ denotes a unit vector from the center-of-mass of the j^{th} face of the i^{th} spacecraft to the Sun, P denotes the mean momentum flux at 1AU, $c_{s,ij}$ is the coefficient of specular reflection of the j^{th} face of the i^{th} spacecraft, and $c_{d,ij}$ is the coefficient of diffuse reflection of face j of the i^{th} spacecraft.

4. Formation Guidance Design

The formation guidance algorithm has two functions: (1) planning relative positions of the follower spacecraft so that the desired electromagnetic beam pattern is attained, and (2) planning fuel-optimal, collision-free reconfiguration trajectories to form new beam patterns or balance fuel consumption. The first guidance function requires optimal aperture positioning (a genetic-algorithm based approach is presently under study), and a prescribed set of relative spacecraft positions is used for this purpose.

The second guidance function has been designed and implemented using two different algorithms. The first algorithm is applicable to formations in circular orbits, and is based on linearized Lambert targeting (LLT) using the Hill-Clohessy-Wiltshire (HCW) equations discussed below. The collision avoidance algorithm for LLT guidance is heuristic-based, and is not guaranteed to converge to collision-free trajectories nor is it optimal. However, the LLT algorithm is a quick and efficient method for calculating reconfigurations. The second reconfiguration guidance algorithm is an implementation of the linear programming (LP) algorithm of [15]. The LP algorithm is applicable to formations in eccentric orbits. However, it is optimal only when the fleet leader is fixed on a reference orbit. The LP algorithm first discretizes the control input and then minimizes the absolute value of the acceleration for a spacecraft reconfiguration. For our purposes, the main benefit of the LP algorithm is the ability to enforce state constraints for collision avoidance.

5. Formation Control Design

5.1. Translational Control

Since our primary goal is to develop a general formation controller to support sparse aperture beam pattern analysis/optimization over a wide range of formation orbits, a classical design method was chosen for developing the individual spacecraft translational control-laws. Classical design methods have straightforward robustness criteria and have proven to perform adequately even when design assumptions are violated. The control design-model is based on the HCW equations, which describe the relative (linearized) translational dynamics between a leader and follower spacecraft when they are near a circular orbit. The reference frame and variables used in the HCW equations are shown in Figure 5. The HCW frame has an origin O traveling on a circular reference orbit and coordinate axes $\hat{x}_h, \hat{y}_h$, and $\hat{z}_h$ where $\hat{y}_h$ is parallel to the circular orbit velocity, $\hat{z}_h$ is perpendicular to the orbital plane, and $\hat{x}_h$ completes the right-handed triad. The HCW frame is also rotating with constant angular velocity $\vec{\omega}_0 = \omega_0 \hat{z}_h$. The position of the leader in the HCW frame is given by $\vec{\rho}_j$ and the position of the follower by $\vec{\rho}_i$. The position of the leader with respect to the follower, resolved in the HCW frame, is given by $\rho_{ij} = [x \quad y \quad z]^T$. When both $|\vec{\rho}_j|$ and $|\vec{\rho}_i|$ are small compared to the orbital radius, the equations of motion are

$$\ddot{x} - 3\omega_0^2 x - 2\omega_0 \dot{y} = a_x \tag{14}$$

$$\ddot{y} + 2\omega_o \dot{x} = a_y \tag{15}$$

$$\ddot{z} + \omega_o^2 z = a_z \tag{16}$$

where a_x, a_y and a_z are inertial accelerations due to all control forces and disturbances resolved in the HCW frame.

Topographic Mission," *IEEE Trans. Geoscience and Remote Sensing*, Vol. 30(1), pp. 103-109, 1992.
[4] Massonnet, D., "Capabilities and Limitations of the Interferometric Cartwheel," *IEEE Trans. Geoscience and Remote Sensing*, Vol. 39(3), pp. 506-520, 2001.
[5] Wang, P.K.C., and Hadaegh, F.Y., "Coordination and Control of Multiple Microspacecraft Moving in Formation," *J. of the Astronautical Sci.*, Vol. 44(3), pp. 315-355, 1996.
[6] Crassidis, J.L., Lightsey, E.G., and Markley, F.L., "Efficient and Optimal Attitude Determination Using Recursive Global Positioning System Signal Operation," *J. Guidance, Control, and Dynamics*, Vol. 22 (2), pp. 193-201, 199.
[7] Maciejowski, J.M., Multivariable Feedback Design, Addison-Wesley Publishing Company: Wokingham, England, 1989.
[8] Hovd, M., Braatz, R.D., and Skogestad, S., "SVD Controllers for H_2-, H_8- and μ -Optimal Control," *American Control Conf.*, 1994.
[9] Tillerson, M., Inalhan, G., and How, J.P., "Co-ordination and Control of Distributed Spacecraft Systems Using Convex Optimization Techniques," *Int. J. of Robust and Nonlinear Control*, Vol. 12, pp. 207-242, 2002.
[10] Singh, G. and Hadaegh, F.Y., "Collision Avoidance Guidance for Formation-Flying Applications," *AIAA Guidance, Navigation, and Control Conf.*, 2001.
[11] Gendreau, K.C., White, N., Owens, S., Cash, W., Shipley, A., and Joy, M., "The MAXIM X-ray Interferometry Mission Concept Study," *36th Liege Int. Astrophysics Colloquium*, Liege, Belgium, 2001.
[12] Beichman, C.A., "The Terrestrial Planet Finder: The Search for Life-Bearing Planets Around Other Stars," *SPIE Conference on Astronomical Interferometry*, Kona, Hawaii, 1998.
[13] Bauer, F.H., Hartman, K., and Lightsey, E.G., "Spacebourne GPS Current Status and Future Visions," *IEEE Aerospace Conf.*, 1998.

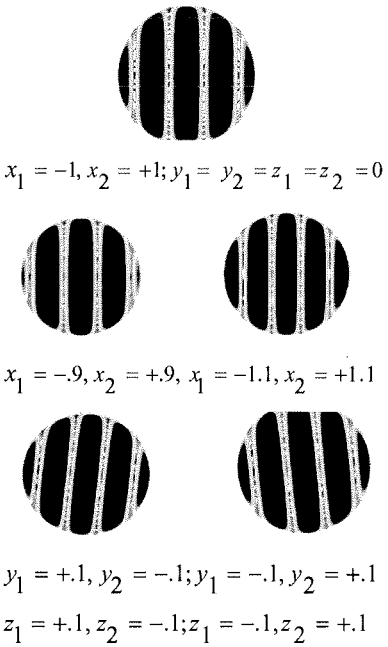

Figure 6. Beam Contour Variations

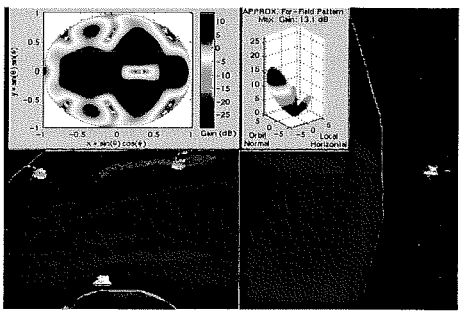

Figure 7. Simulation testbed GUI

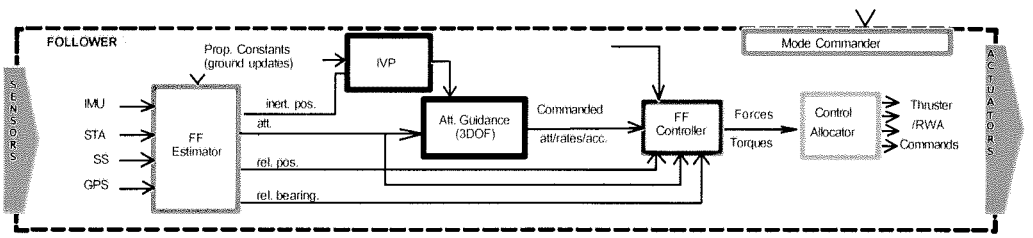

Figure 8. Formation G&C architecture